Electronic Supplementary Material (ESI) for Physical Chemistry Chemical Physics.

SUPPLEMENTARY INFORMATION

Sandwich-type $Na_6B_7^-$ and $Na_8B_7^+$ clusters: Charge-transfer complexes, four-fold π/σ aromaticity, and dynamic fluxionality†

Ying-Jin Wang,‡[a,b] Lin-Yan Feng,‡[b] and Hua-Jin Zhai*[b]

[a]*Department of Chemistry, Xinzhou Teachers University, Xinzhou 034000, China*

[b]*Nanocluster Laboratory, Institute of Molecular Science, Shanxi University, Taiyuan 030006, China*

*E-mail: hj.zhai@sxu.edu.cn

Supplementary Information – Part I

Table S1. Cartesian coordinates for the global-minimum (GM) structures of $Na_6B_7^-$ (**1**, D_{3d}, $^1A_{1g}$) and $Na_8B_7^+$ (**5**, D_{3d}, $^1A_{1g}$) clusters at the PBE0/6-311+G* level.

Figure S1. Alternative low-lying structures of $Na_6B_7^-$ cluster. Relative energies at the PBE0/6-311+G* level are shown in square brackets, with corrections for zero-point energies (ZPEs). Also shown are energies for top low-lying isomers at the single-point CCSD(T)/6-311G*//PBE0/6-311+G* level. All energies are in eV.

Figure S2. Alternative low-lying structures of $Na_8B_7^+$ cluster. Relative energies at the PBE0/6-311+G* level are shown in square brackets, with corrections for ZPEs. Also shown are energies for top low-lying isomers at the single-point CCSD(T)/6-311G*//PBE0/6-311+G* level. All energies are in eV.

Figure S3. Structural evolution of $Na_8B_7^+$ cluster during the dynamic rotations. Two pathways are available via transition states **6** and **7**, which are denoted as TS_1 and

TS_2, respectively. Each pathway is associated to a soft vibrational mode of $Na_8B_7^+$ cluster. The lower pathway is related to free rotation of B_7 wheel against two Na_4 subunits, while the upper one is due to twisting between two Na_4 subunits.

Figure S4. Calculated bond distances (in Å; black color), Wiberg bond indices (WBIs; blue color), and natural atomic charges (in |e|; red color) for (a) $Na_6B_7^-$ (**2**, TS_1), (b) $Na_6B_7^-$ (**3**, TS_2), and (c) $Na_6B_7^-$ (**4**, LM). Here TS and LM represent transition state and local minimum, respectively. WBIs and natural atomic charges are obtained from natural bond orbital (NBO) analyses at the PBE0/6-311G* level.

Figure S5. Calculated bond distances (in Å; black color), WBIs (blue color), and natural atomic charges (in |e|; red color) for (a) $Na_8B_7^+$ (**6**, TS_1), (b) $Na_8B_7^+$ (**7**, TS_2), and (c) $Na_8B_7^+$ (**8**, LM). WBIs and natural atomic charges are obtained from the NBO analyses at the PBE0/6-311G* level.

Figure S6. Canonical molecular orbitals (CMOs) of D_{3d} (**5**, $^1A_{1g}$) GM structure of $Na_8B_7^+$ cluster. (a) Six σ CMOs for peripheral two-center two-electron (2c-2e) B–B σ bonds in the B_7 wheel. (b) Three delocalized σ CMOs. (c) Three delocalized π CMOs. (d) Two delocalized σ CMOs over two Na_4 tetrahedra. Subsystems (b) through (d) collectively render four-fold (2σ/6π/6σ/2σ) aromaticity for $Na_8B_7^+$ cluster.

Figure S7. Occupied CMOs of the D_{3d} (**2**, $^1A_{1g}$) TS_1 structure for $Na_6B_7^-$ cluster. The CMOs are similar to those in Figs. 4 and S6, except for a slight spatial shift of the electron clouds, which does not alter the essence of chemical bonding.

Figure S8. Bonding pattern of the D_{3d} (**2**, $^1A_{1g}$) TS_1 structure for $Na_6B_7^-$ cluster on the basis of adaptive natural density partitioning (AdNDP) analysis. Occupation numbers (ONs) are indicated.

Figure S9. Occupied CMOs of the D_{3h} (**4**, $^1A_1'$) LM structure for $Na_6B_7^-$ cluster. The CMOs are similar to those in Figs. 4, S6, and S7, except for a slight spatial shift of the electron clouds, which does not alter the essence of chemical bonding.

Figure S10. AdNDP bonding pattern of the D_{3h} (**4**, $^1A_1'$) LM structure for $Na_6B_7^-$ cluster. ONs are indicated.

Figure S11. Simulated photoelectron spectrum of $Na_6B_7^-$ cluster at the time-dependent PBE0/6-311+G* (TD-PBE0) level. The simulation was conducted using the D_{3d} (**1**, $^1A_{1g}$) GM structure by fitting the calculated vertical detachment energies (VDEs) with unit-area Gaussian functions of 0.02 eV half-width.

Supplementary Information – Part II

A short movie extracted from the BOMD simulation for $Na_6B_7^-$ cluster. The simulation was performed at 300 K for 50 ps. The movie roughly covers a time span of 8 ps. Similar BOMD properties have been probed for $Na_8B_7^+$ cluster at 300 K (not shown).

Figure S1. Alternative low-lying structures of $Na_6B_7^-$ cluster. Relative energies at the PBE0/6-311+G* level are shown in square brackets, with corrections for zero-point energies (ZPEs). Also shown are energies for top low-lying isomers at the single-point CCSD(T)/6-311G*//PBE0/6-311+G* level. All energies are in eV.

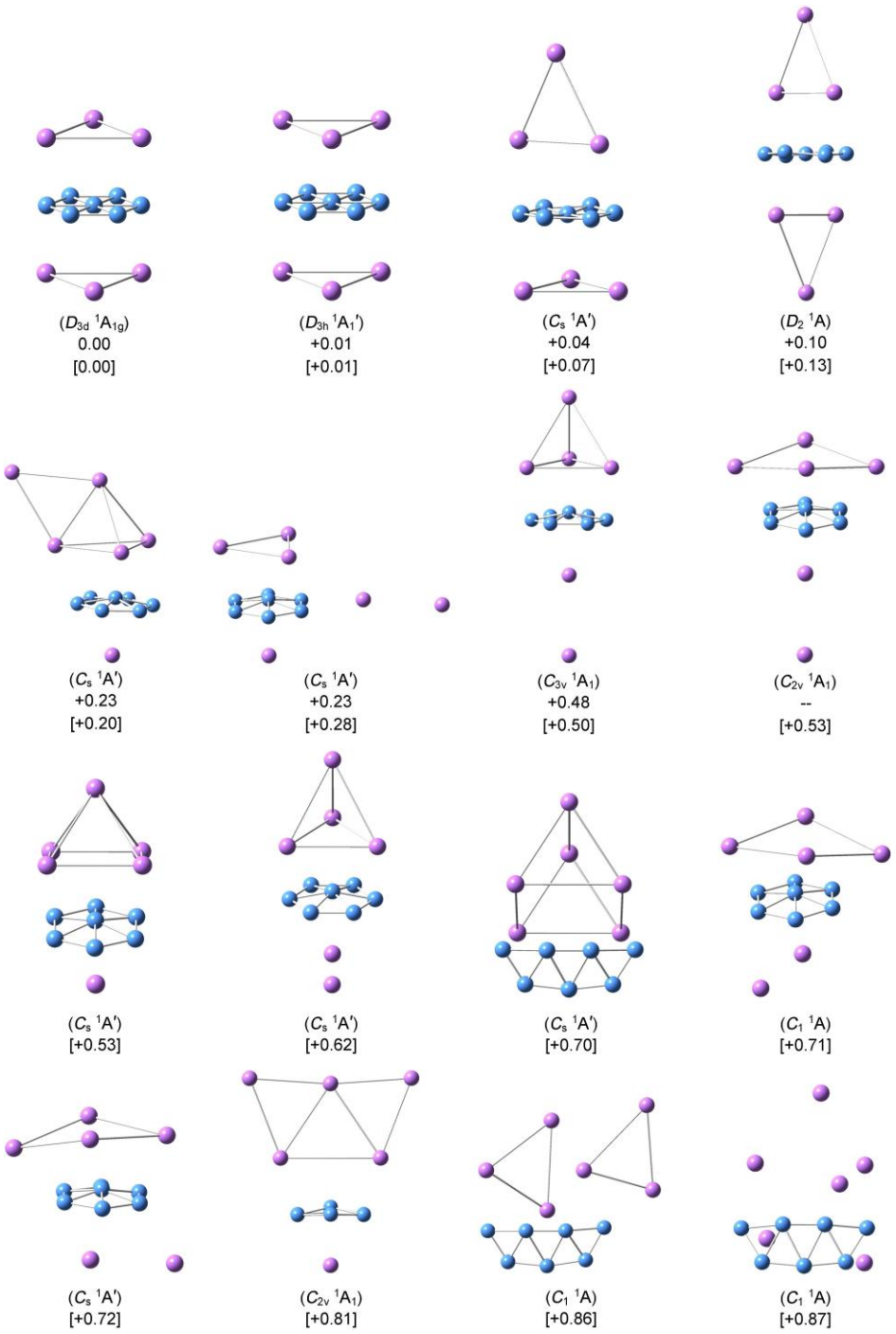

(… continued)

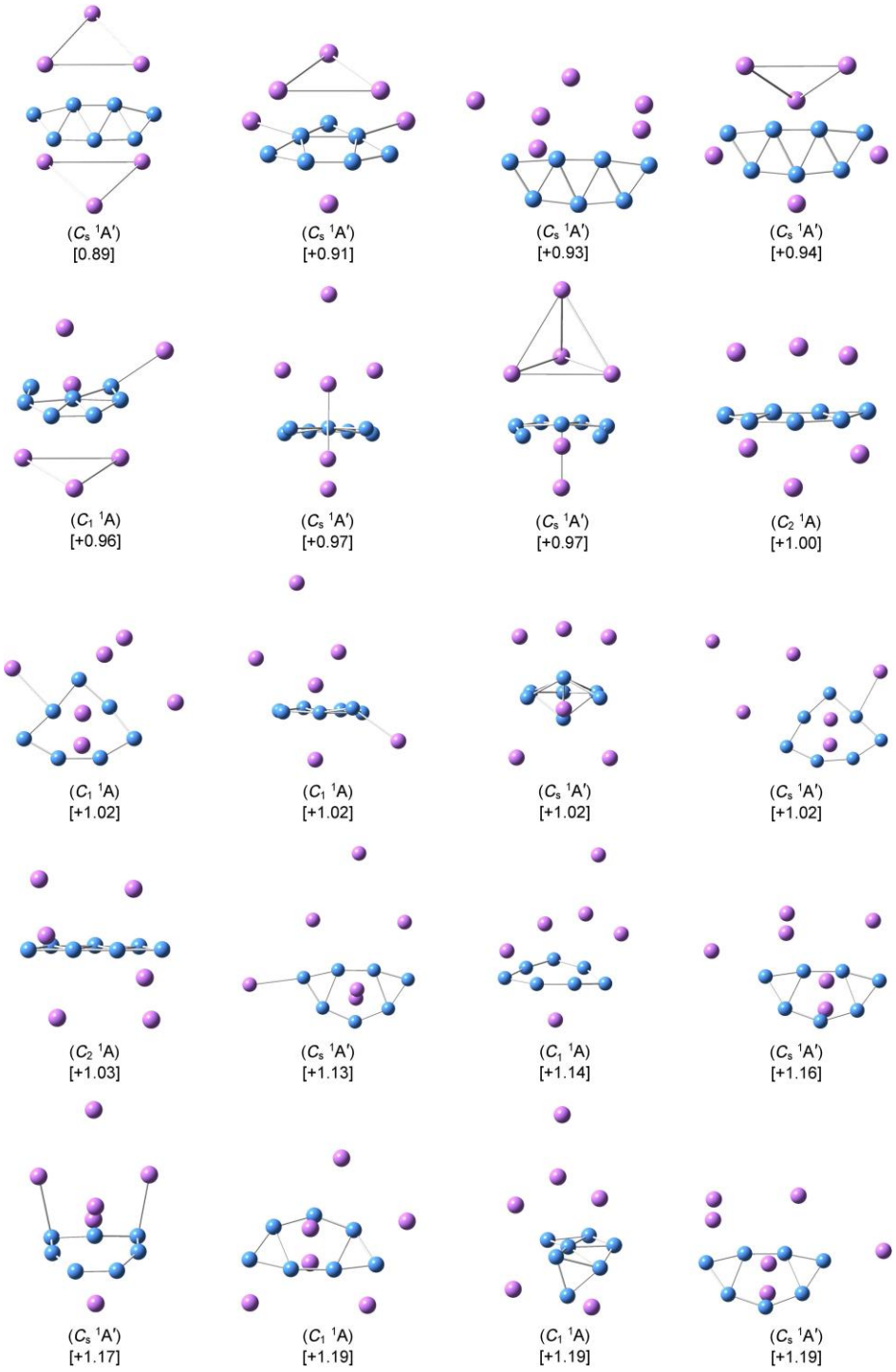
(C_s ^{1}A′)
[0.89]
(C_s ^{1}A′)
[+0.91]
(C_s ^{1}A′)
[+0.93]
(C_s ^{1}A′)
[+0.94]
(C_1 ^{1}A)
[+0.96]
(C_s ^{1}A′)
[+0.97]
(C_s ^{1}A′)
[+0.97]
(C_2 ^{1}A)
[+1.00]
(C_1 ^{1}A)
[+1.02]
(C_1 ^{1}A)
[+1.02]
(C_s ^{1}A′)
[+1.02]
(C_s ^{1}A′)
[+1.02]
(C_2 ^{1}A)
[+1.03]
(C_s ^{1}A′)
[+1.13]
(C_1 ^{1}A)
[+1.14]
(C_s ^{1}A′)
[+1.16]
(C_s ^{1}A′)
[+1.17]
(C_1 ^{1}A)
[+1.19]
(C_1 ^{1}A)
[+1.19]
(C_s ^{1}A′)
[+1.19]

Figure S2. Alternative low-lying structures of $Na_8B_7^+$ cluster. Relative energies at the PBE0/6-311+G* level are shown in square brackets, with corrections for ZPEs. Also shown are energies for top low-lying isomers at the single-point CCSD(T)/6-311G*//PBE0/6-311+G* level. All energies are in eV.

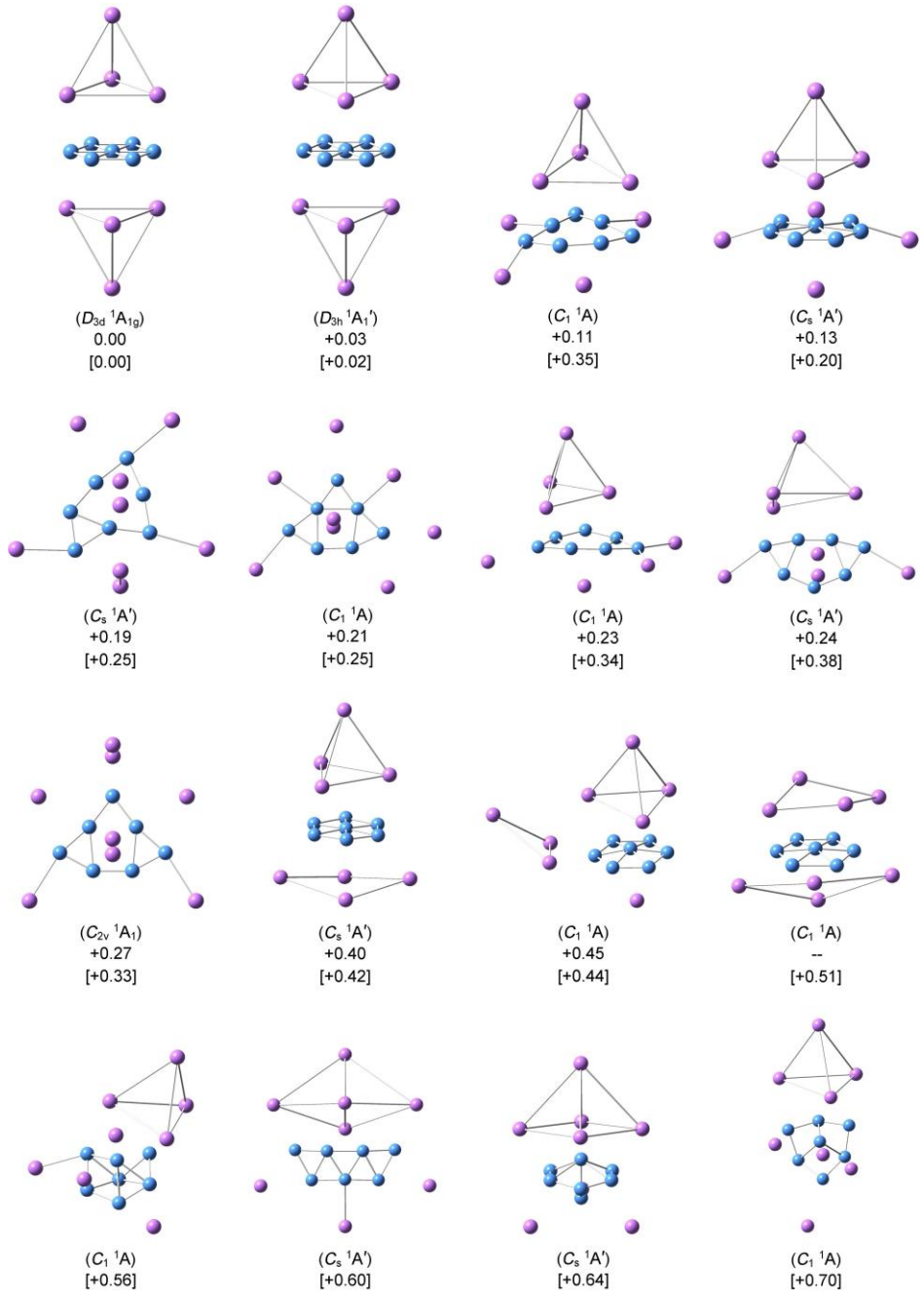

(… continued)

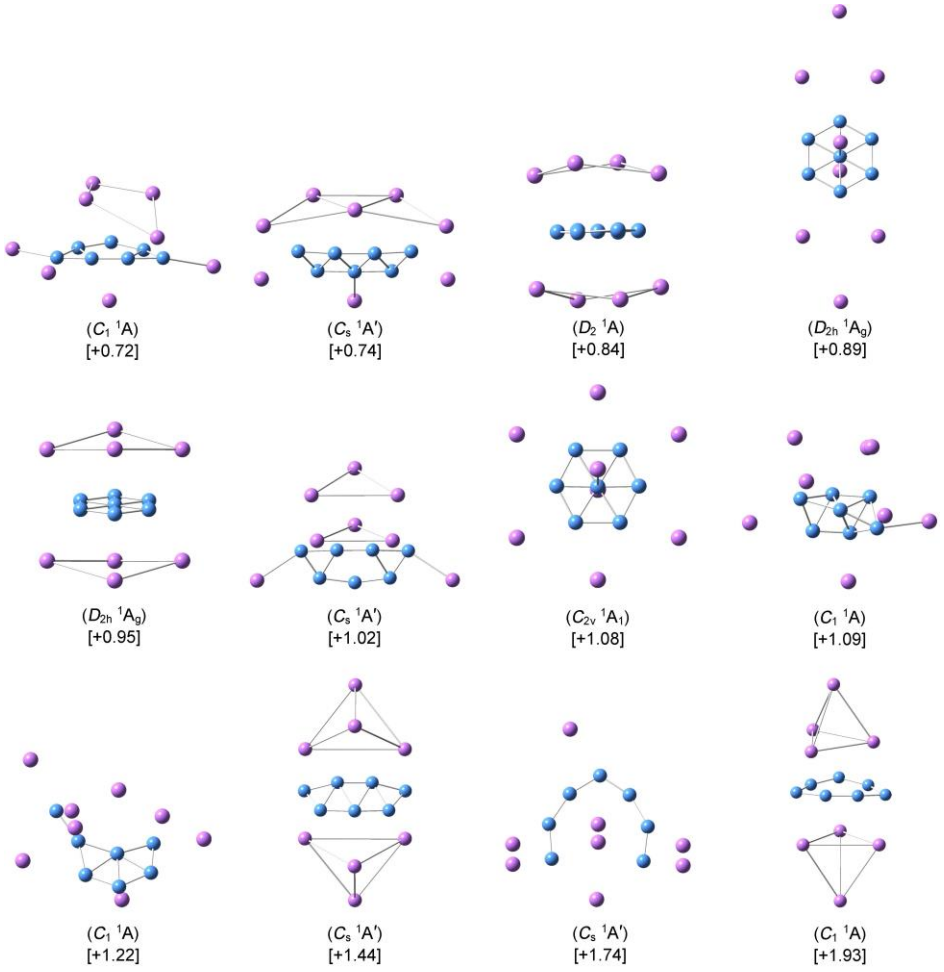
(C_1 ^{1}A)
[+0.72]
(C_s ^{1}A′)
[+0.74]
(D_2 ^{1}A)
[+0.84]
(D_{2h} ^1A_g)
[+0.89]
(D_{2h} ^1A_g)
[+0.95]
(C_s ^{1}A′)
[+1.02]
(C_{2v} $^1A_1$)
[+1.08]
(C_1 ^{1}A)
[+1.09]
(C_1 ^{1}A)
[+1.22]
(C_s ^{1}A′)
[+1.44]
(C_s ^{1}A′)
[+1.74]
(C_1 ^{1}A)
[+1.93]

Figure S3. Structural evolution of $Na_8B_7^+$ cluster during the dynamic rotations. Two pathways are available via transition states **6** and **7**, which are denoted as TS_1 and TS_2, respectively. Each pathway is associated to a soft vibrational mode of $Na_8B_7^+$ cluster. The lower pathway is related to free rotation of B_7 wheel against two Na_4 subunits, while the upper one is due to twisting between two Na_4 subunits.

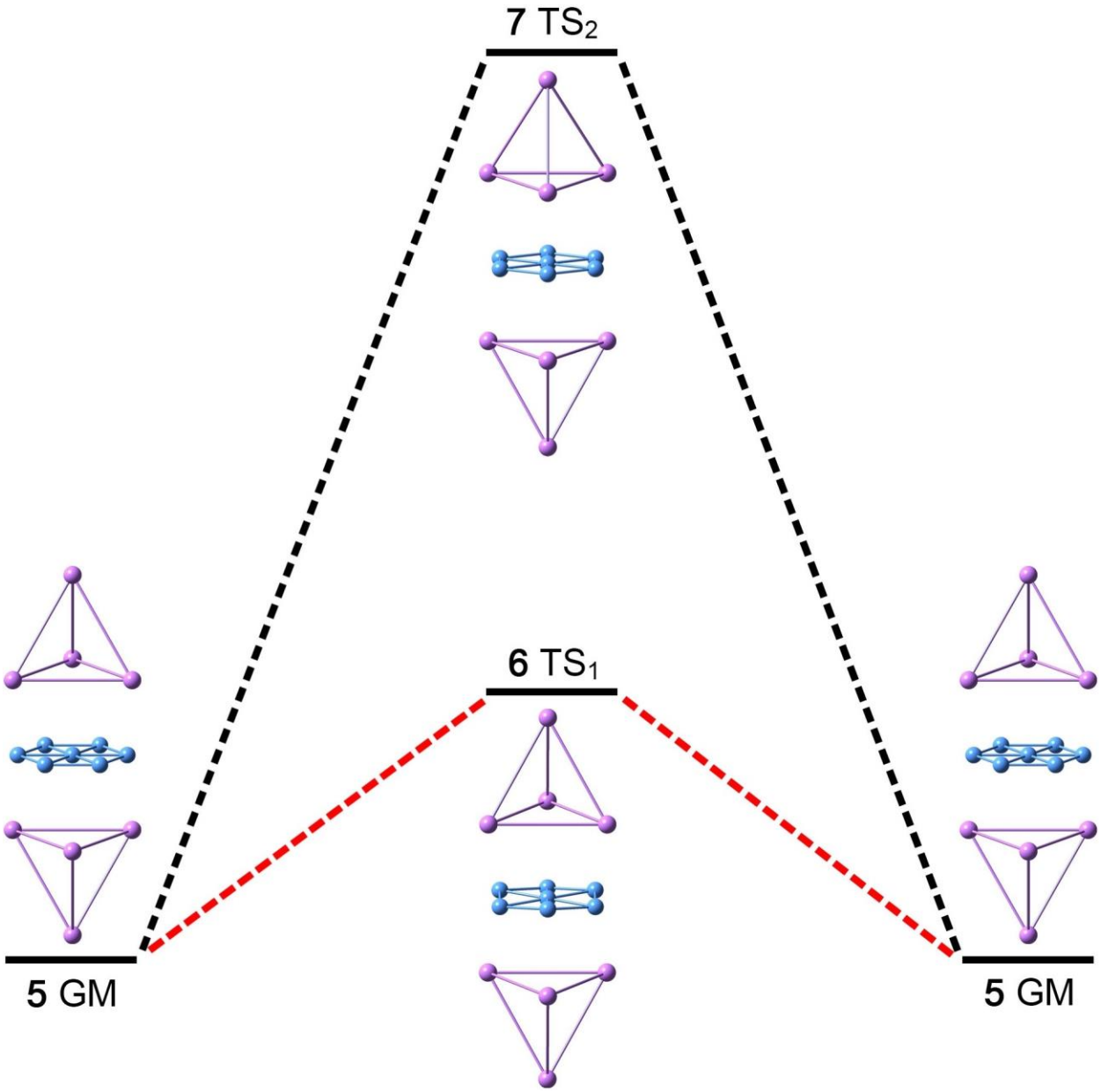

Figure S4. Calculated bond distances (in Å; black color), Wiberg bond indices (WBIs; blue color), and natural atomic charges (in |e|; red color) for (a) $Na_6B_7^-$ (**2**, TS_1), (b) $Na_6B_7^-$ (**3**, TS_2), and (c) $Na_6B_7^-$ (**4**, LM). Here TS and LM represent transition state and local minimum, respectively. WBIs and natural atomic charges are obtained from natural bond orbital (NBO) analyses at the PBE0/6-311G* level.

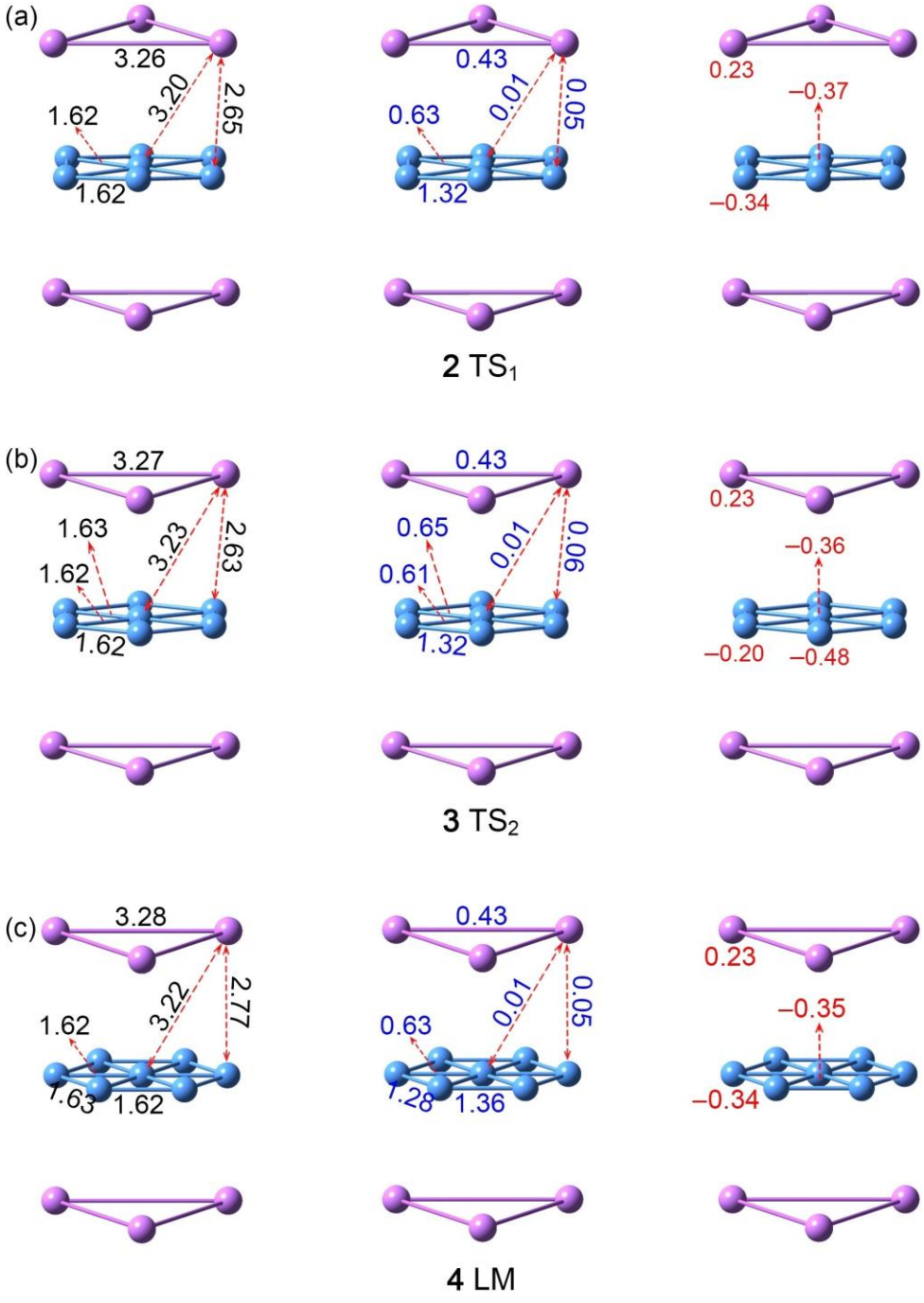

Figure S5. Calculated bond distances (in Å; black color), WBIs (blue color), and natural atomic charges (in |e|; red color) for (a) $Na_8B_7^+$ (**6**, TS_1), (b) $Na_8B_7^+$ (**7**, TS_2), and (c) $Na_8B_7^+$ (**8**, LM). WBIs and natural atomic charges are obtained from the NBO analyses at the PBE0/6-311G* level.

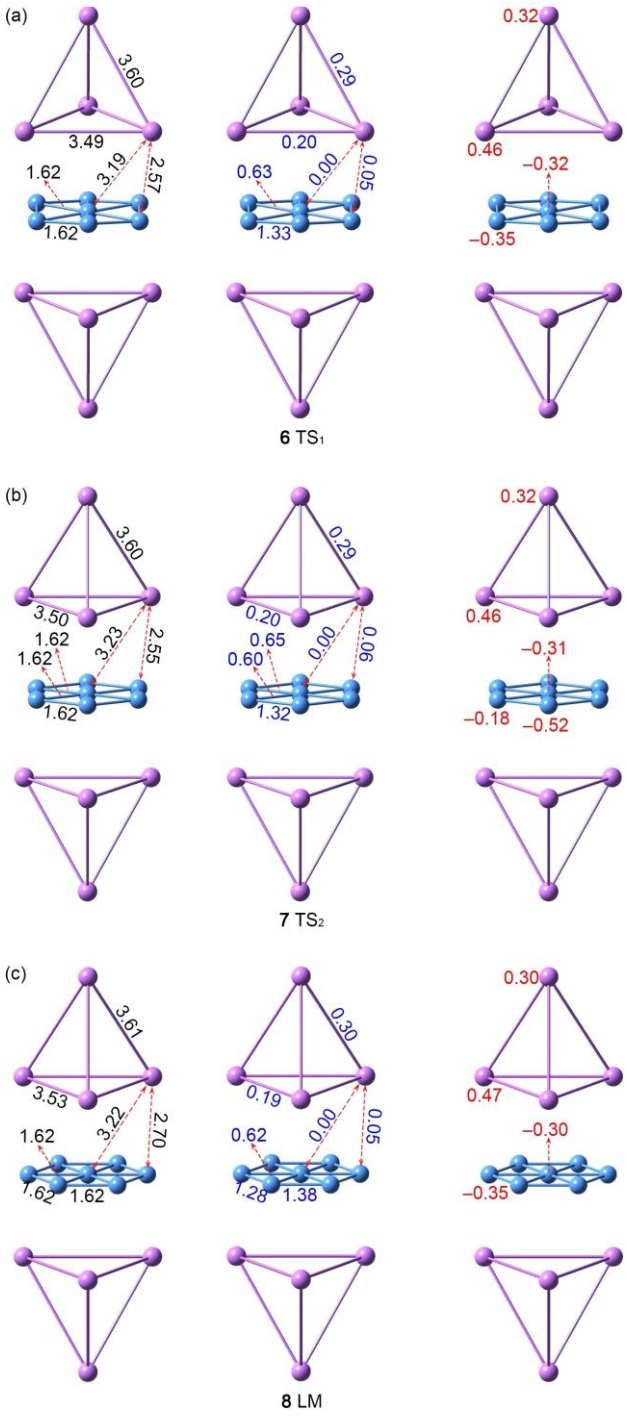

Figure S6. Canonical molecular orbitals (CMOs) of D_{3d} (**5**, $^1A_{1g}$) GM structure of $Na_8B_7^+$ cluster. (a) Six σ CMOs for peripheral two-center two-electron (2c-2e) B–B σ bonds in the B_7 wheel. (b) Three delocalized σ CMOs. (c) Three delocalized π CMOs. (d) Two delocalized σ CMOs over two Na_4 tetrahedra. Subsystems (b) through (d) collectively render four-fold (2σ/6π/6σ/2σ) aromaticity for $Na_8B_7^+$ cluster.

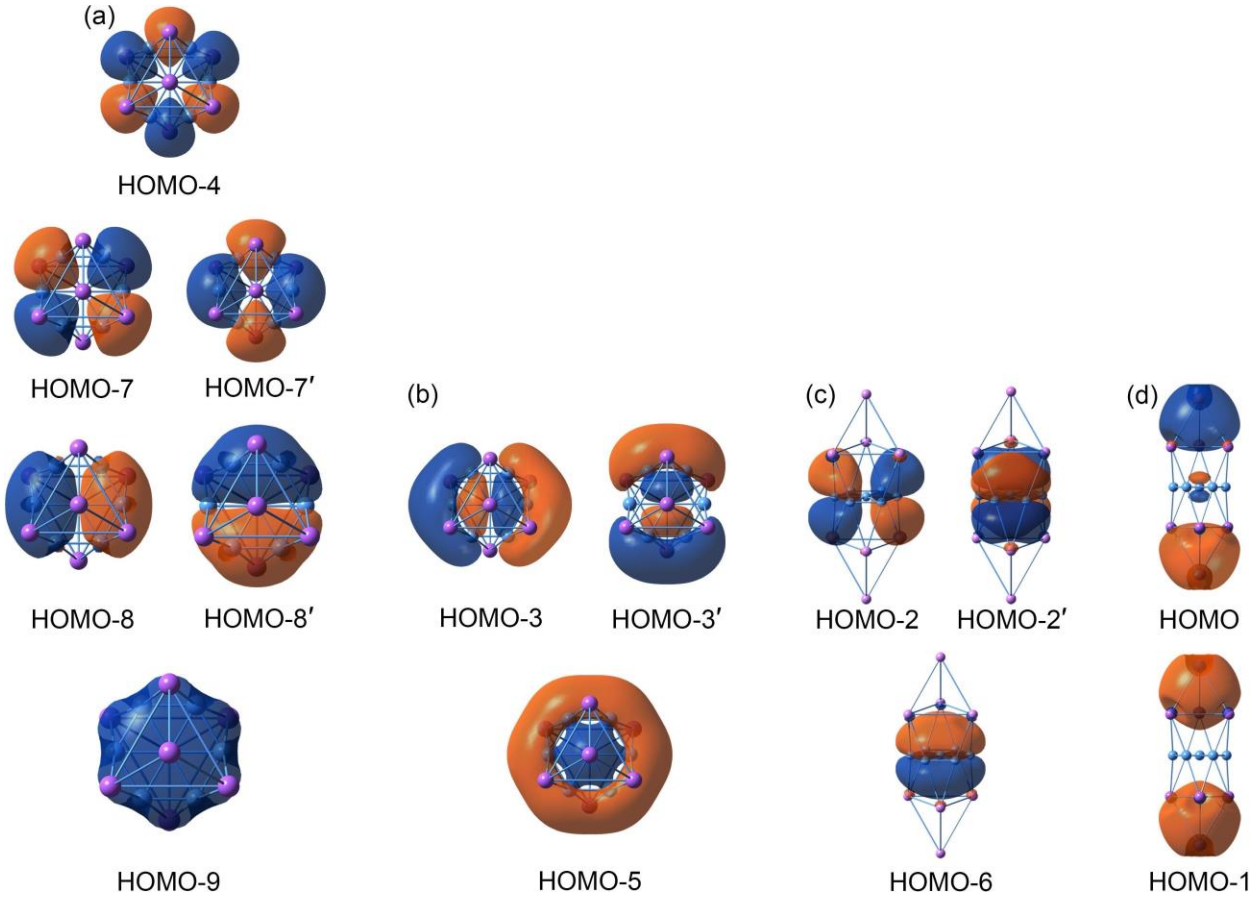

Figure S7. Occupied CMOs of the D_{3d} (**2**, $^1A_{1g}$) TS_1 structure for $Na_6B_7^-$ cluster. The CMOs are similar to those in Figs. 4 and S6, except for a slight spatial shift of the electron clouds, which does not alter the essence of chemical bonding.

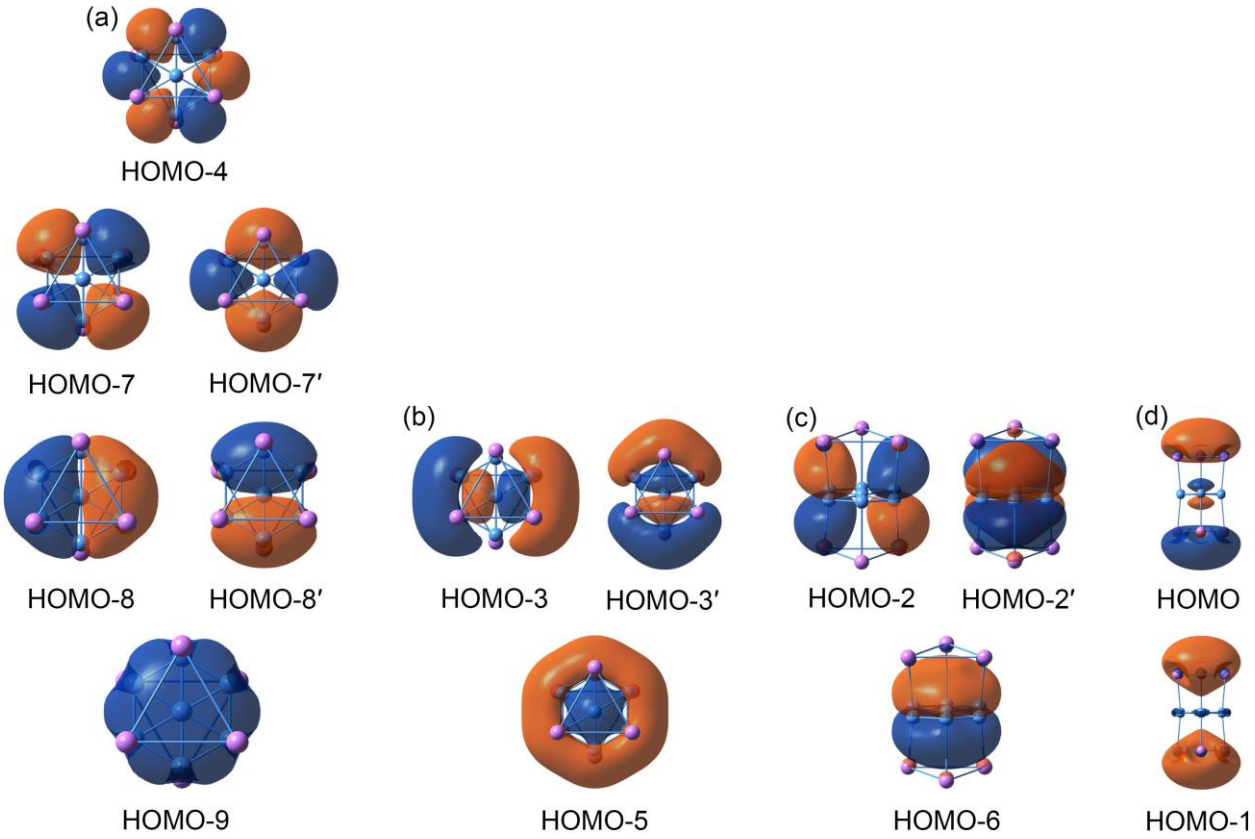

Figure S8. Bonding pattern of the D_{3d} (**2**, $^1A_{1g}$) TS_1 structure for $Na_6B_7^-$ cluster on the basis of adaptive natural density partitioning (AdNDP) analysis. Occupation numbers (ONs) are indicated.

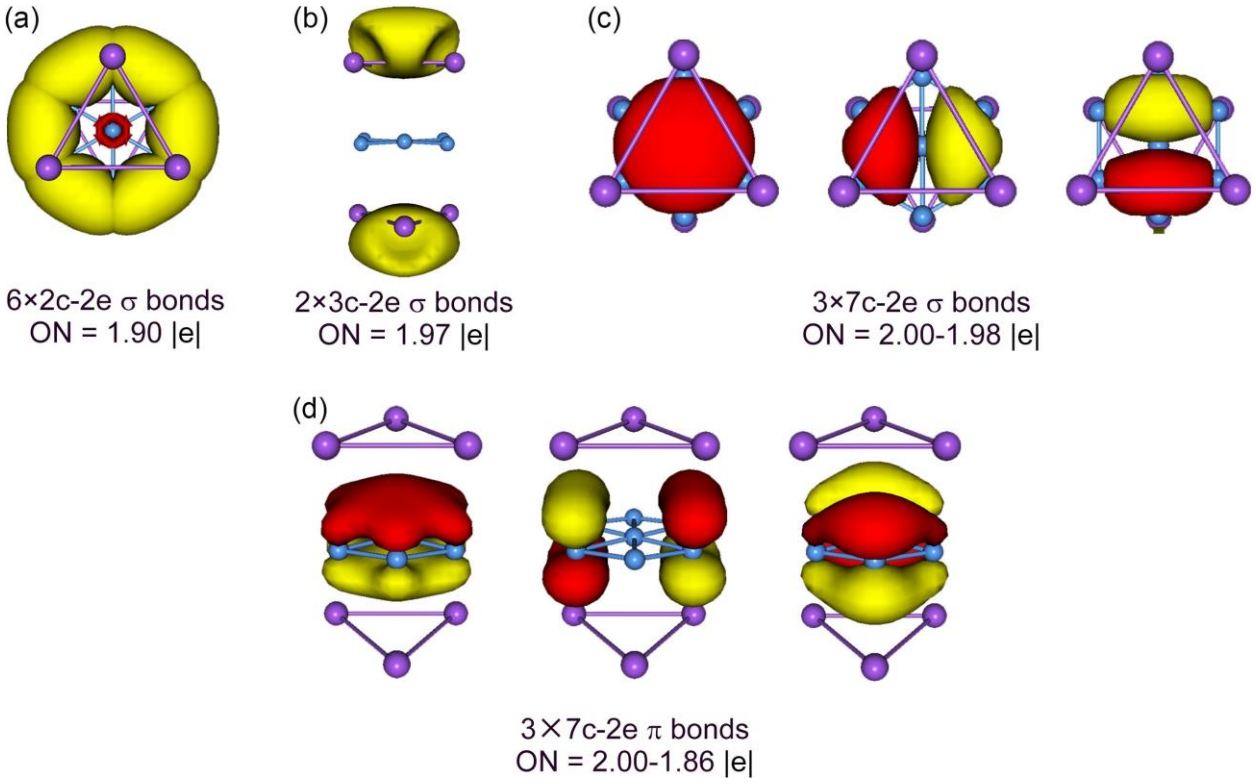

Figure S9. Occupied CMOs of the D_{3h} (**4**, $^1A_1'$) LM structure for $Na_6B_7^-$ cluster. The CMOs are similar to those in Figs. 4, S6, and S7, except for a slight spatial shift of the electron clouds, which does not alter the essence of chemical bonding.

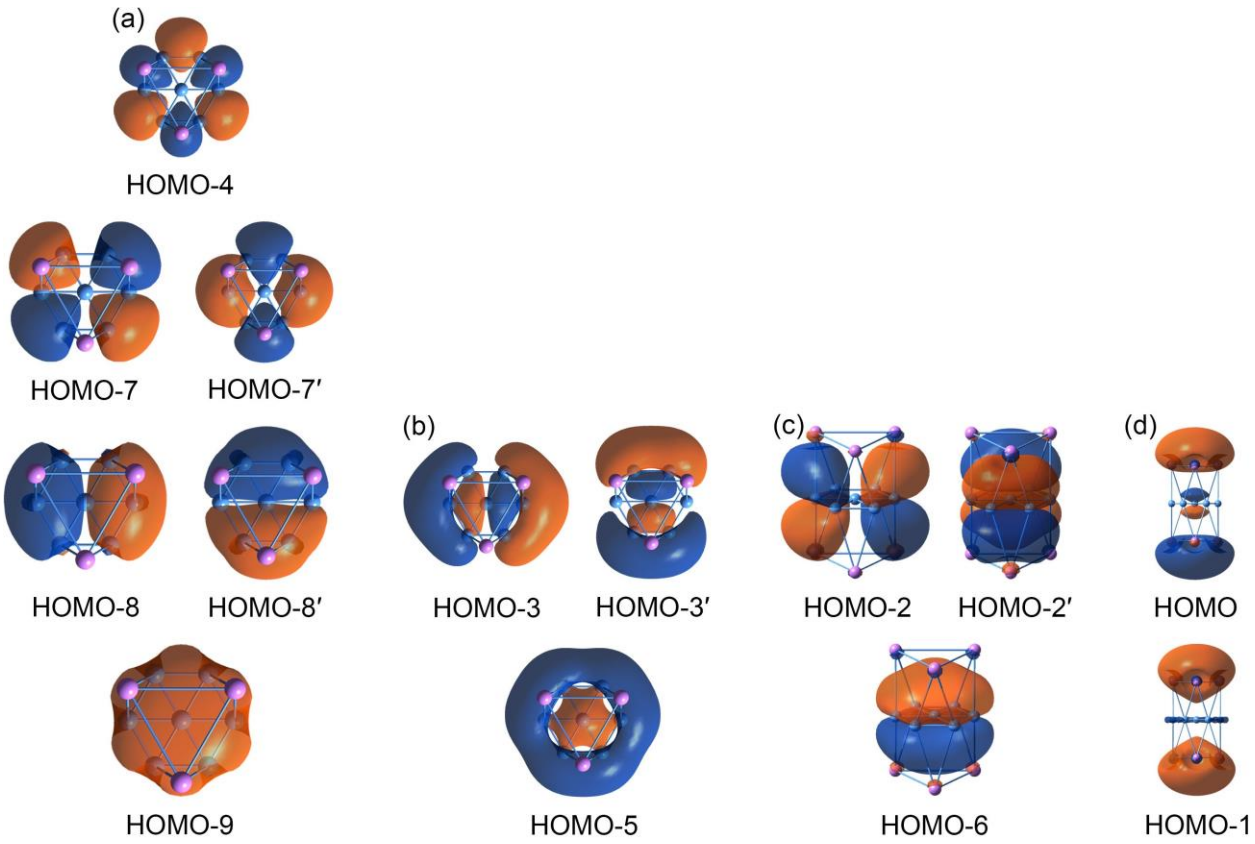

Figure S10. AdNDP bonding pattern of the D_{3h} (**4**, $^1A_1'$) LM structure for $Na_6B_7^-$ cluster. ONs are indicated.

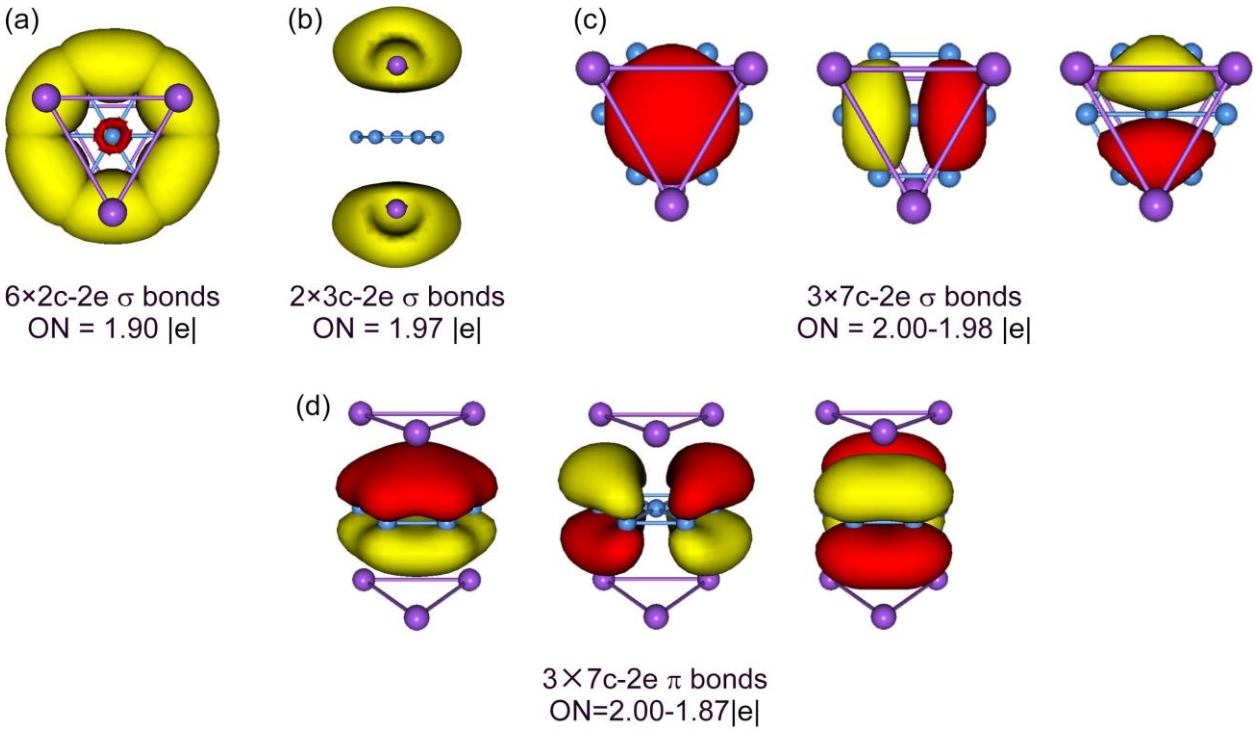

Figure S11. Simulated photoelectron spectrum of $Na_6B_7^-$ cluster at the time-dependent PBE0/6-311+G* (TD-PBE0) level. The simulation was conducted using the D_{3d} (**1**, $^1A_{1g}$) GM structure by fitting the calculated vertical detachment energies (VDEs) with unit-area Gaussian functions of 0.02 eV half-width.

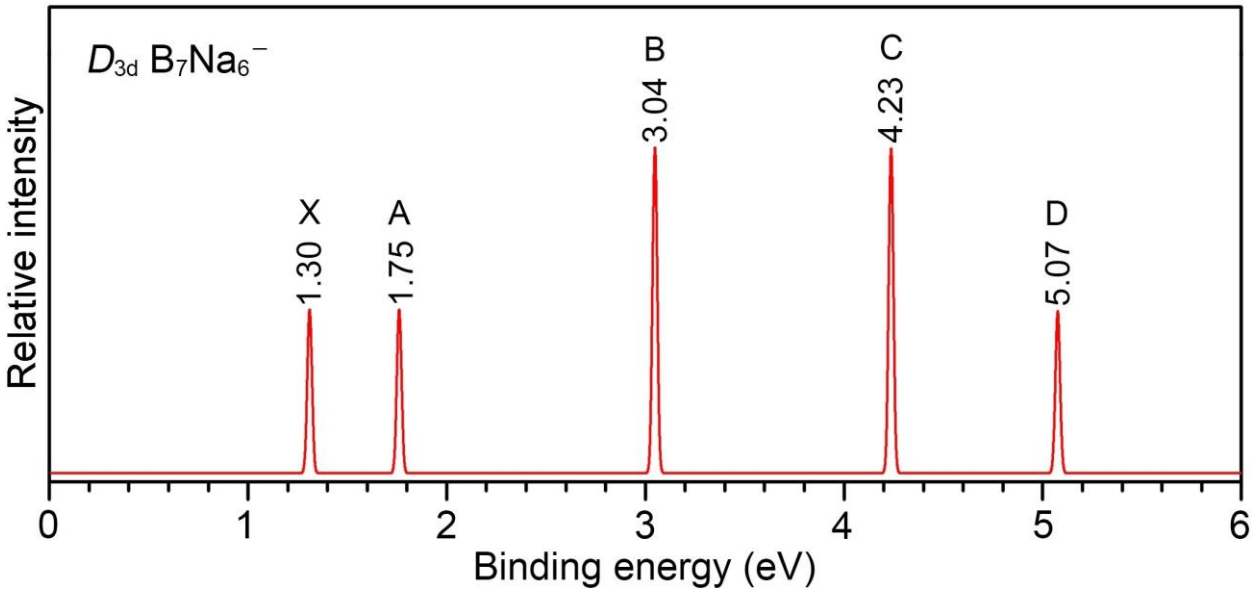

Table S1. Cartesian coordinates for the global-minimum (GM) structures of $Na_6B_7^-$ (**1**, D_{3d}, $^1A_{1g}$) and $Na_8B_7^+$ (**5**, D_{3d}, $^1A_{1g}$) clusters at the PBE0/6-311+G* level.

(a) GM, $Na_6B_7^-$ (**1**, D_{3d}, $^1A_{1g}$)

B	0.81156285	1.40566809	0.00000000
B	-0.81156285	1.40566809	0.00000000
B	0.81156285	-1.40566809	0.00000000
B	-0.81156285	-1.40566809	0.00000000
B	-1.62312570	-0.00000000	0.00000000
B	1.62312570	0.00000000	0.00000000
B	0.00000000	0.00000000	0.00000000
Na	1.64088312	0.94736431	2.59772681
Na	-0.00000000	1.89472862	-2.59772681
Na	-1.64088312	0.94736431	2.59772681
Na	-1.64088312	-0.94736431	-2.59772681
Na	0.00000000	-1.89472862	2.59772681
Na	1.64088312	-0.94736431	-2.59772681

(b) GM, $Na_8B_7^+$ (**5**, D_{3d}, $^1A_{1g}$)

B	0.81035200	1.40357100	0.00000000
B	-0.81035200	1.40357100	0.00000000
B	0.81035200	-1.40357100	0.00000000
B	-0.81035200	-1.40357100	0.00000000
B	-1.62070400	0.00000000	0.00000000
B	1.62070400	0.00000000	0.00000000
B	0.00000000	0.00000000	0.00000000
Na	1.76725100	1.02032300	2.48933400

Na	0.00000000	2.04064600	-2.48933400
Na	-1.76725100	1.02032300	2.48933400
Na	-1.76725100	-1.02032300	-2.48933400
Na	0.00000000	-2.04064600	2.48933400
Na	1.76725100	-1.02032300	-2.48933400
Na	0.00000000	0.00000000	5.46523900
Na	0.00000000	0.00000000	-5.46523900